JACS
JOURNAL OF THE AMERICAN CHEMICAL SOCIETY

ARTICLE

pubs.acs.org/JACS

Protein Micro- and Nanopatterning Using Aminosilanes with Protein-Resistant Photolabile Protecting Groups

Shahrul A. Alang Ahmad,[†,∥,#] Lu Shin Wong,[§,∥] Ehtsham ul-Haq,[†,‡] Jamie K. Hobbs,[†,‡] Graham J. Leggett,[*,†] and Jason Micklefield[*,§]

[†]Department of Chemistry, University of Sheffield, Brook Hill, Sheffield S3 7HF, United Kingdom

[‡]Department of Physics and Astronomy, University of Sheffield, Hicks Building, Hounsfield Road, Sheffield S3 7RH, United Kingdom

[§]School of Chemistry & Manchester Interdisciplinary Biocentre, The University of Manchester, 131 Princess Street, Manchester M1 7DN, United Kingdom

Supporting Information

ABSTRACT: An approach to the integration of nanolithography with synthetic chemical methodology is described, in which near-field optical techniques are used to selectively deprotect films formed by the adsorption of aminosilanes protected by modified 2-nitrophenylethoxycarbonyl (NPEOC) groups. The NPEOC groups are functionalized at the *m*- or *p*-position with either a tetraethyleneglycol or a heptaethylene glycol adduct. We describe the synthesis of these bioresistant aminosilanes and the characterization of the resulting photoreactive films. Photodeprotection by exposure to UV light (λ = 325 nm) yielded the amine with high efficiency, at a similar rate for all four adsorbates, and was complete after an exposure of 2.24 J cm^{-2}. Following photodeprotection, derivatization by trifluoroacetic anhydride was carried out with high efficiency. Micropatterned samples, formed using a mask, were derivatized with aldehyde-functionalized polymer nanoparticles and, following derivatization with biotin, were used to form patterns of avidin-coated polymer particles. Fluorescence microscopy and atomic force microscopy data demonstrated that the intact protecting groups conferred excellent resistance to nonspecific adsorption. Nanometer-scale patterns were created using scanning near-field photolithography and were derivatized with biotin. Subsequent conjugation with avidin-functionalized polymer nanoparticles yielded clear fluorescence images that indicated dense attachment to the nanostructures and excellent protein resistance on the surrounding surface. These simple photocleavable protecting group strategies, combined with the use of near-field exposure, offer excellent prospects for the control of surface reactivity at nanometer resolution in biological systems and offer promise for integrating the top-down and bottom-up molecular fabrication paradigms.

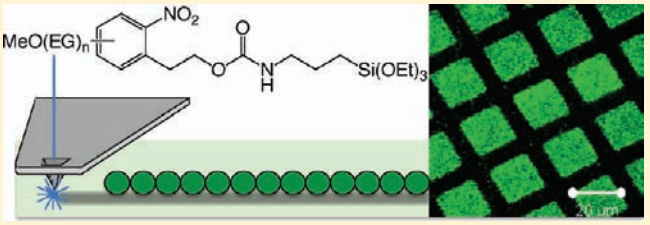

INTRODUCTION

The integration of top-down (lithographic) with bottom-up (synthetic chemical) approaches remains a central challenge in nanofabrication. The majority of work on molecular nanopatterning has utilized physical methods for the deposition[1−5] or removal[6−8] of material, with subsequent elaboration of structures formed this way being possible via a variety of routes (for example, host−guest chemistry[9] or interactions between Ni-NTA and His-tagged proteins[10]). However, the development of tools for the direct initiation of specific chemical transformations on nanometer length scales would add a new dimension to the construction of nanostructured assemblies. The importance of this was recognized by Sagiv and co-workers,[11,12] who used a potential difference applied between an AFM tip and a surface to drive oxidative modification of silane films. Subsequently, a number of approaches to the excitation of specific chemical pathways have been reported, including methods based upon electrochemistry,[13] nanopipettes,[14] and the use of tip-immobilized enzymes,[15] catalytically active metals,[16,17] and metal nanoparticles[18] to catalyze surface reactions. However, for the full integration of synthetic chemical methodology into a top-down framework, we require generalized methodologies that permit the creation, on demand, of a range of surface molecular architectures.

Photochemical methods have a long-standing and well-established place in synthetic chemical methodology. The development of light-directed chemical synthesis[19] by Fodor et al. enabled the translation of synthetic chemical methodology into microtechnology, by exploiting photolithography, in combination with the deployment of highly efficient photocleavable protecting groups, to carry out spatially defined solid-phase synthesis. The use of light for this purpose is appealing because it enables "reagent-free" deprotections and allows a high degree of spatial registry. Such approaches have proved enormously valuable in oligonucleotide synthesis[20] and form the basis for the solid-phase fabrication of DNA chips by sequential photodeprotection-base coupling steps.[21−23]

Light-directed synthesis thus provides a model for the integration of top-down and bottom-up fabrication methods. The main drawback is the limited resolution of conventional far-field

Received: November 18, 2010
Published: February 8, 2011

dx.doi.org/10.1021/ja1103662 | J. Am. Chem. Soc. 2011, 133, 2749–2759

optical techniques. However, extensive work in the authors' laboratories has demonstrated that near-field optical techniques enable the translation of photochemical patterning to the nanometer scale,[24,25] because evanescent (near) fields are not subject to the diffraction effects that limit the resolution of conventional optical methods. In scanning near-field photolithography (SNP), a UV laser coupled to a scanning near-field optical microscope is used to initiate photochemical reactions. Using SNP, structures as small as 9 nm have been fabricated in self-assembled monolayers (SAMs) of alkylthiolates on gold.[26] The methodology has subsequently been extended to a wide range of other materials including monolayers of alkylsiloxanes[27] and phosphonic acids,[28,29] as well as films of polymers,[30,31] metallic nanoparticles.[32] and fullerenes.[33] Recently, we described new approaches to the parallelization of near-field lithography, with a device (the "Snomipede") that uses parallel near-field exposure to execute photodeprotection steps in organic films and can achieve a spatial resolution of 70 nm with an array of probes immersed under water.[34]

To fully integrate top-down and bottom-up approaches, it is necessary to develop generic protecting group strategies that enable the photoswitchable or photoactivatable introduction of a wide range of functional groups to surfaces. Nitrophenyl-based protecting groups are very promising in this respect. The *o*-nitroveratryloxycarbonyl (NVOC)[35] and α-methyl-*o*-nitropiperonyloxycarbonyl (MeNPOC)[36−38] groups are now well established in synthetic chemistry and are suitable for the protection of carboxy and hydroxy moieties, while the recently introduced nitrophenylpropyloxycarbonyl (NPPOC) protecting group[20,39] may be used to protect amines and yields an exceptionally high photodeprotection efficiency.[40] MeNPOC caging of biotinylated surfaces has been used in micrometer scale biological patterning,[41] while Nakayama et al. attached biotin to a nitrophenyl photocleavable linker, enabling its selective removal from surfaces.[42] In a different approach, Alonso et al. synthesized an NVOC protected aminosilane, which, following photodeprotection, was derivatized with tris-nitrilo triacetic acid (tris-NTA), enabling the immobilization of His-tagged proteins.[43] Other promising avenues offering generic surface functionalization capability include the use of thiol−ene reactions[44,45] and photoactivated click reactions.[46] These results highlight the power of photochemistry for carrying out organic synthesis at surfaces. However, none of these papers has demonstrated molecular patterning with nanometer-scale spatial resolution. In efforts to merge the versatility of this synthetic chemistry and the spatial resolution of near-field photolithography, we recently reported the synthesis of NPPOC-protected aminopropyltriethoxysilane and demonstrated that nanometer-scale patterns may readily be generated by using a near-field probe to expose the adsorbates.[47] These deprotected amine groups could subsequently undergo a variety of chemical manipulations including acetylations and imine formation.

Nanometer-scale biological structures offer the potential for addressing a plethora of scientific problems, including the development of ultrasensitive detection systems for biological diagnostics[48−57] and fundamental studies of mechanisms of cellular attachment.[5,53,58−61] However, biological systems present several important and difficult issues for nanofabrication including, in particular, nonspecific adsorption (fouling). Proteins are particularly challenging in this regard because they adsorb strongly and irreversibly to most surfaces. At nanometer length scales, biomolecules are on a comparable size scale to the nanofabricated features, and any undesired adsorption results in a significant degradation in resolution and performance. Hence, any strategy for the integration of top-down and bottom up methodologies that is to be capable of use for biomolecular nanofabrication must also address the important problem of nonspecific adsorption. Ideally for the fabrication of materials with integrated biomolecules, a surface is required that is bioresistant and chemically passive, yet switchable to a surface that is able to undergo further synthetic manipulation upon photoirradiation.

In the present work, we have addressed these complex challenges by attaching a nitrophenylethoxycarbonyl protecting group to aminopropyltriethoxysilane, because amine groups (formed by photodeprotection) are a convenient basis for subsequent solid-phase synthesis. We demonstrate the reactivity of deprotected amines by coupling biotin using a succinimidyl ester derivative, although the free amine offers a generic point from which many other bioconjugation strategies are accessible. To prevent nonspecific adsorption, we have functionalized the phenyl ring with protein-resistant oligoethylene glycol chains.[62−66] For alkylthiolate SAMs, a minimum of three ethylene glycol (EG) units is required to ensure protein resistance.[67] Because siloxane films are known to exhibit lower order and a wider distance between neighboring headgroups compared to alkylthiol SAMs, we have compared protecting groups functionalized with four and seven EG units, to ensure complete coverage of the underlying surface. Further, because the effect of the OEG attachment on the photochemistry of the nitrophenylethyloxycarbonyl group is unknown, we have additionally compared molecules with OEG substituents located *m*- and *p*- to the nitro group.

RESULTS AND DISCUSSION

Synthesis of Photoreactive Silanes. The syntheses of all the photoreactive silanes were completed following a similar route (Scheme 1). Initially, monomethoxy oligoethylene glycols **1a,b** were first tosylated[68,69] and then treated with the appropriate methylnitrophenol isomers to give **2a−d** in good yields. These were then converted to the alcohols **3a−d** with paraformaldehyde under KO^{t}Bu catalysis in DMSO.[70] Unlike previous reports with the NPPOC and related photolabile groups,[40,47,71] the use of Triton B as the base did not yield any desired product in all cases. For **3a−c**, these were then coupled with 3-isocyanatopropyltriethoxysilane[47] to give the desired products **4a−c**. However, **4d** was found to be inseparable from the *N*,*N*′-di(3-triethoxysilylpropyl)urea side product. This was instead prepared through the intermediate formation of the 4-nitrophenyl carbonate followed by reaction with 3-aminopropyltriethoxysilane in a one-pot two-step sequence.

Film Formation and Characterization. Films were formed from the nitrophenylethyoxycarbonyl-protected aminopropyltriethoxysilanes **4a−d**, henceforth NPEOC-APTES. The advancing water contact angles of all four films were in close agreement, falling in the range 43.8−44.9° (Table 1). The differences between the values obtained for the films were small as compared to the experimental error, suggesting that the composition of the surface presented by all four adsorbate films is similar.

Film thicknesses were measured using ellipsometry. Films of tetraethyleneglycol NPEOC-APTES (EG_4NPEOC-APTES) were ca. 6 nm thick, making them fractionally thicker than the films of NPPOC-APTES reported in an earlier study (5.5 nm),[47]

Table 1. Contact Angle and Ellipsometry Data for Films of Photosenstive Silanes

	protecting group			
	m-EG_4NPEOC (from **4a**)	*p*-EG_4NPEOC (**4b**)	*m*-EG_7NPEOC (**4c**)	*p*-EG_7NPEOC (**4d**)
θ_a/deg	44.9 ± 1.5	44.5 ± 0.9	43.1 ± 0.8	43.8 ± 0.8
ellipsometric thickness/nm	5.7 ± 0.30	6.3 ± 0.3	9.2 ± 1.1	8.9 ± 0.5

Scheme 1. Sy nthesis of Photoreactive Silanes[a]

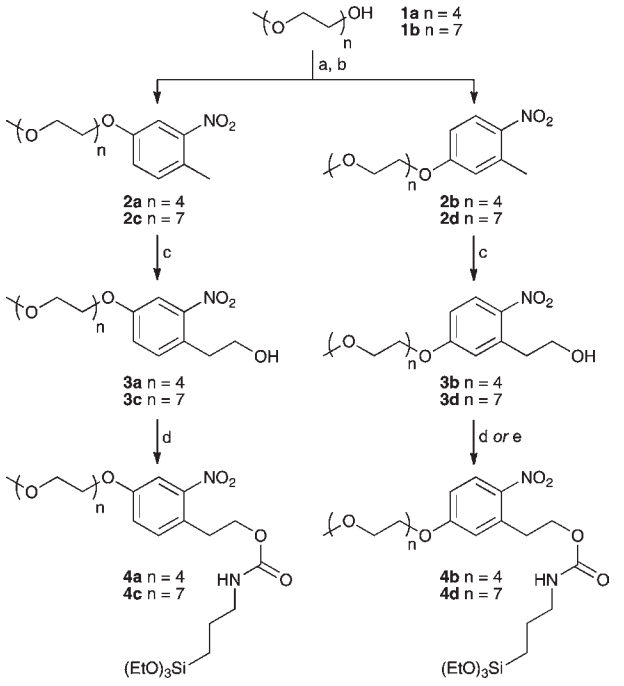

[a] Reagents and conditions: (a) TsCl, NaOH, THF/H_2O, 3 h, 84% (**1a**) or 70% (**1b**); (b) 4-methyl-3-nitrophenol or 3-methyl-4-nitrophenol, K_2CO_3, acetone (**2a**−**c**) or DCM (**2d**), reflux, 6 h (**2a** and **2b**) or 16 h (**2c** and **2d**), 91% (**2a**) or 88% (**2b**) or 89% (**2c**) or 84% (**2d**); (c) paraformaldehyde, KO^tBu (cat.), DMSO, 80 °C, 30 min, 35% (**3a**) or 34% (**3b**) or 25% (**3c**) or 30% (**3d**); (d) 3-isocyanatopropyltriethoxysilane, Et_3N (cat.), DCM, reflux, 24 h, 63% (**4a**) or 62% (**4b**) or 65% (**4c**); (e) 4-nitrophenol chloroformate, Et_3N, DCM, 6 h, then 3-aminopropyltriethoxysilane, EtOH/DCM, 16 h, 30% (**4d** over two steps).

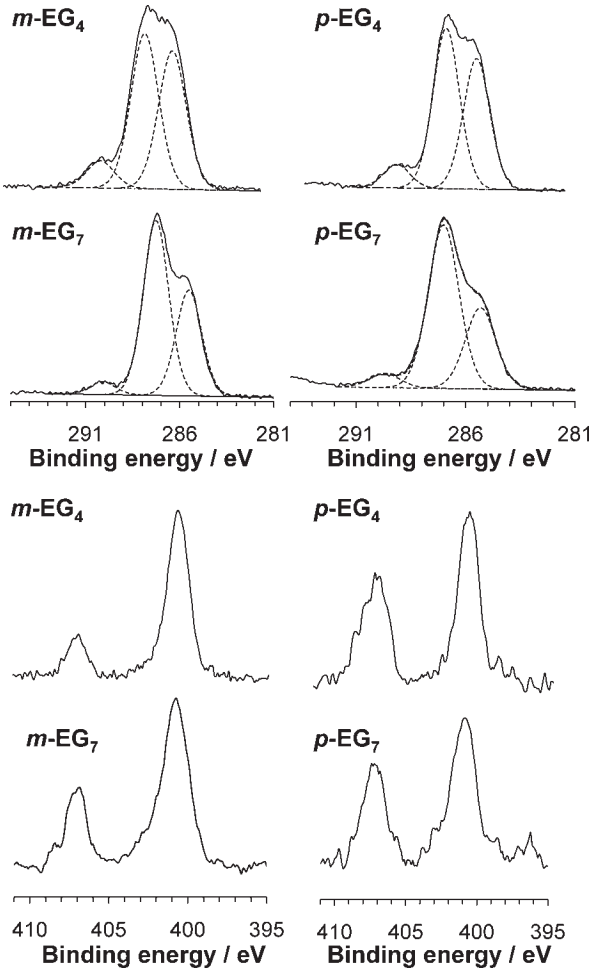

Figure 1. C 1s (top) and N 1s (bottom) photoelectron spectra for EG_nNPEOC-APTES monolayers.

which were estimated to be ca. two molecular layers thick. EG_4NPEOC-APTES **4a** and **4b** are longer than NPPOC-APTES, by approximately the length of the EG_4 unit, estimated to be ca. 1 nm. Hence, it may be concluded that the EG_4NPEOC-APTES films were also close to bilayer thickness, on average. Films of EG_7NPEOC-APTES **4c** and **4d** were thicker than films of EG_4NPEOC-APTES by ca. 3 nm, consistent with the formation of a film of bilayer thickness, given the greater length of the heptaethylene glycol adducts. These data are consistent with the well-documented tendency of silanes to self-polymerize, and in general to form more disordered films than comparable alkylthiolates on gold. The film thicknesses reported here were highly reproducible under the conditions used.

X-ray photoelectron spectra were acquired for all four films. Figure 1 shows the C 1s and N 1s spectra. There are two dominant peaks in each C 1s spectrum: the main hydrocarbon peak at 285 eV, corresponding to the carbon atoms in the aromatic ring, the carbon adjacent to it, and the propyl chain; and a peak at ca. 1.5 eV higher binding energy corresponding to the carbon atoms in the EG tail and also the carbon next to the nitrogen of the carbamate group. There is additionally a component corresponding to the carbonyl carbon atom. In each case, the ether peak was slightly larger than anticipated, based on the molecular formula of the adsorbate, because of attenuation of the photoelectrons emitted from the underlying carbon atoms.

The N 1s spectra exhibited two components at binding energies of ca. 401 and 407 eV, attributed to the carbamate and nitro group nitrogen atoms, respectively. On the basis of consideration of the molecular formulas of the adsorbates, these components would be expected to exhibit the same areas. However, the nitro group component was smaller than the carbamate component in all spectra. The samples were all stored in the dark so photodeprotection was unlikely. Rather, the observation was attributed to X-ray-induced modification of the samples during analysis. To confirm that this was the case, and that deprotection of adsorbates did not occur during storage,

dx.doi.org/10.1021/ja1103662 |*J. Am. Chem. Soc.* 2011, 133, 2749–2759

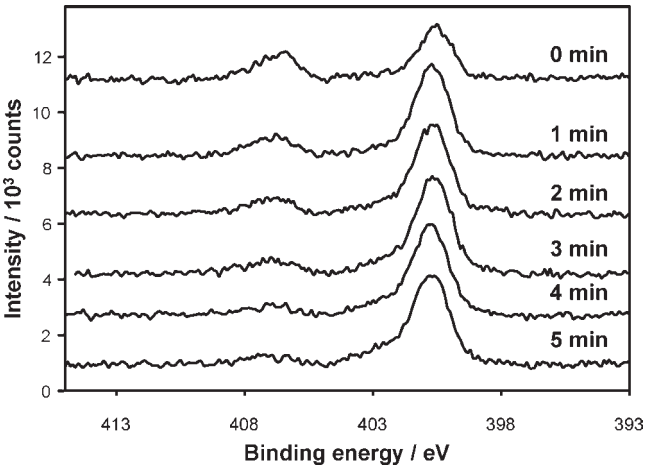

Figure 2. N 1s photoelectron spectra following exposure to UV light for *m*-EG$_7$NPEOC-APTES.

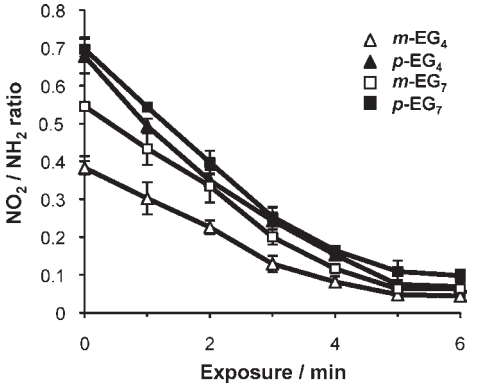

Figure 3. Variation in the ratio of the areas of the nitro and carbamate/amine components in the N 1s spectra of films formed from EG$_n$NPEOC-APTES.

samples were incubated with trifluoroacetic anhydride (TFAA), and their contact angles were measured. The values obtained were analytically identical to those of the films before incubation, suggesting no derivatization had occurred and hence that no deprotection of the adsorbates had occurred. In contrast, after photodeprotection, significant changes were observed in the contact angle following reaction with TFAA (see below). It has been reported that nitrophenyl groups are reduced rapidly upon exposure to X-rays and electrons,[72] and this has been used successfully as a means of patterning nitrophenyl SAMs.[73] The reduced area of the nitro components in the N 1s spectra is here attributed to a similar process. A similar although much less pronounced effect was also observed with the NPPOC-APTES that we previously reported.[47]

Photodeprotection. Figure 2 shows the evolution of the N 1s region of the XPS spectrum with UV exposure for *m*-EG$_7$NPEOC-APTES. The nitro component was visible in the spectrum of the virgin material but quickly declined following exposure to UV light, and after 5 min exposure (1.86 J cm^{-2}) the intensity of this component was very much reduced.

The N1 s spectra of the other three adsorbates exhibited very similar qualitative changes as a function of exposure. To quantitatively compare the behavior of the four adsorbates, the ratio of the nitro peak to the main peak (representing the sum of the carbamate component for the unmodified adsorbate and the amine component following deprotection) was measured as a function of the UV exposure time (Figure 3). The ratio is less than unity for the virgin materials, as described above. Further, the limiting value reached at long exposures was not zero. Taken together with the elipsometry data, which indicate that the average thickness of the assembled films corresponded to two layers of siloxanes, this result suggests that the top layer may be partially preventing the removal of the EG$_n$NPEOC groups in underlying layer. For all four adsorbates, a limiting value was reached after 6 min (2.24 J cm^{-2}), and the rate of change was similar in all four cases.

To confirm that deprotection of the adsorbates was occurring, samples were derivatized in two different ways. First, deprotected

Table 2. Contact Angles of Films Formed from EG$_n$NPEOC-APTES Following UV Exposure and Derivatization with TFAA in THF

protecting group	θ_a/virgin film	θ_a/3 min exposure	θ_a/5 min exposure
m-EG$_4$NPEOC (from **4a**)	46.3 ± 2.5	68.3 ± 2.1	92.0 ± 3.4
p-EG$_4$NPEOC (**4b**)	45.3 ± 2.1	69.7 ± 1.2	89.4 ± 2.1
m-EG$_7$NPEOC (**4c**)	44.0 ± 1.0	66.5 ± 1.5	87.5 ± 4.0
p-EG$_7$NPEOC (**4d**)	45.0 ± 1.0	65.3 ± 3.5	88.8 ± 2.5

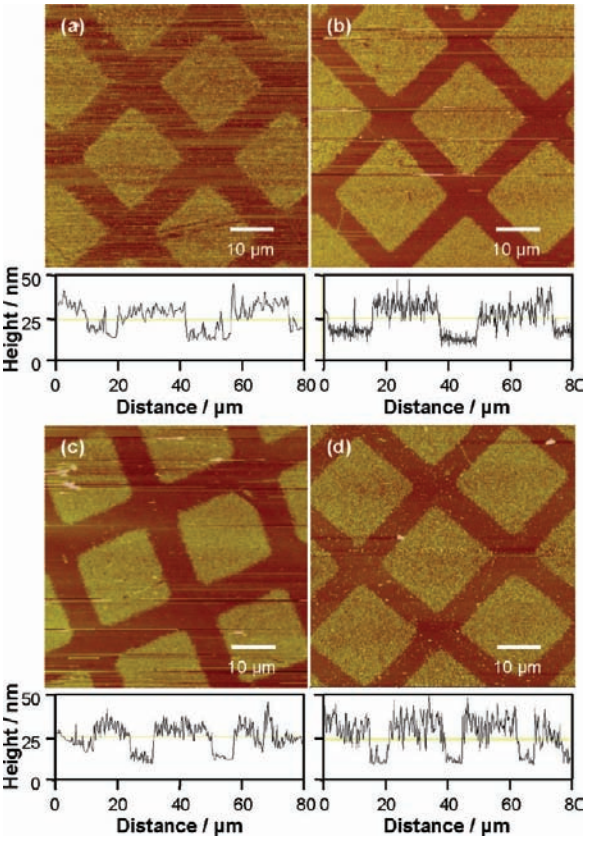

Figure 4. Tapping mode AFM images, and representative line sections, showing micropatterns formed by deprotection of films with different protecting groups through a mask and subsequent derivatization with aldehyde-functionalized polymer nanoparticles. (a) *m*-EG$_4$NPEOC; (b) *m*-EG$_7$NPEOC; (c) *p*-EG$_4$NPEOC; (d) *p*-EG$_7$NPEOC. Vertical scale range: 0−100 nm dark to light.

dx.doi.org/10.1021/ja1103662 |*J. Am. Chem. Soc.* 2011, 133, 2749–2759

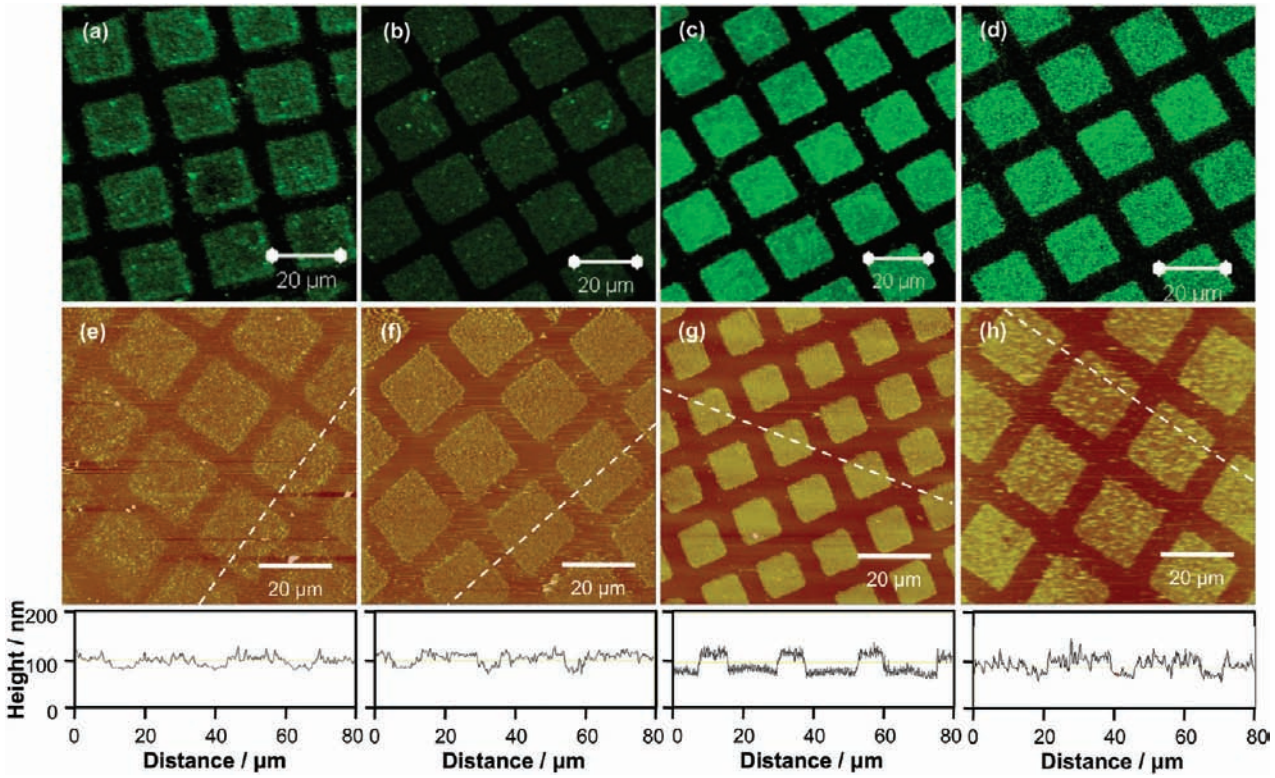

Figure 5. (a−d) Fluorescence micrographs showing micropatterns formed by attachment of NeutrAvidin particles to biotinylated micropatterns formed in films with different protecting groups. (a) *m*-EG_4NPEOC; (b) *p*-EG_4NPEOC; (c) *m*-EG_7NPEOC; (d) *p*-EG_7NPEOC. (e−h) Tapping mode topographical AFM images of micropatterns formed by attachment of NeutrAvidin to biotinylated, deprotected films. (e) *m*-EG_4NPEOC; (f) *p*-EG_4NPEOC; (g) *m*-EG_7NPEOC; (h) *p*-EG_7NPEOC. Cross sections along the dashed lines indicated are shown beneath (e)−(h).

films were immersed in a dilute solution of TFAA in tetrahydrofuran (THF). Reaction between TFAA and the deprotected amine groups yielded an increase in the water contact angle of the film due to the increased hydrophobicity of the trifluoroacetylated surfaces. Table 2 shows data for virgin film (i.e., not exposed to UV light) and films that have been exposed to UV light for 3 and 5 min. The contact angles of the virgin films following exposure to the TFAA solution were very similar to those shown in Table 1, confirming that the protecting groups remained intact, despite the smaller-than-expected size of the nitro component in the N 1s spectra. After 3 min exposure to UV light (1.12 J cm^{-2}), the contact angle rose substantially, to 65−68°, and after 5 min exposure (1.86 J cm^{-2}), the contact angle measured was very similar to that recorded for a control sample, formed by adsorption of APTES onto a silicon dioxide surface.[47] These data indicate that photodeprotection of the films was extensive, in agreement with the data in Figure 3.

Samples were also exposed to UV light through an electron microscope grid, as a simple micrometer-scale photomask, and treated with a solution of aldehyde-functionalized polymer nanoparticles (42 nm diameter). The aldehyde functional groups on the surfaces of the nanoparticles react with the amine groups produced by photodeprotection of EG_nNPEOC-APTES films to form imine bonds, providing topographical contrast and enabling the derivatization to be confirmed by AFM (Figure 4). Clear topographical contrast was evident, with nanoparticles observed to be closely packed across the exposed areas (squares) and not present on the masked regions where the NPEOC protecting groups remained intact. The height of the nanoparticle films on the exposed regions was measured to be ca. 40 nm, consistent with the formation of a monolayer of immobilized nanoparticles in those regions.

Protein Patterning. Deprotected EG_nNPEOC-APTES films were functionalized by biotin molecules attached to *N*-hydroxysuccinimidyl ester-terminated linkers (henceforth NHS-biotin). NeutrAvidin particles (avidin-coated nanoparticles fluorescently labeled with fluorescein isothiocyanate (FITC)) were coupled to the patterns via the specific biotin−avidin recognition interaction, and the samples were imaged using confocal fluorescence microscopy (Figure 5a−d). Adhesion of the NeutrAvidin particles to the surface is dominated by the interactions between the avidin coating and the surface; they thus exhibit adsorption characteristics similar to those of Avidin, but also possess a significant loading of dye (FITC) facilitating imaging by fluorescence microscopy. Bright fluorescence was observed from the exposed regions (squares) where the OEG-functionalized protecting groups had been removed, and dark contrast was observed where the protecting groups were intact.

Tapping mode AFM images (Figure 5e−h) confirmed that nonspecific adsorption onto the unexposed regions was negligible. The NeutrAvidin particles were sufficiently well resolved that they could be readily observed where they did adsorb on the regions covered with intact EG_nNPEOC protecting groups, but only a very small number of isolated particles were detected. In contrast, on the deprotected, biotinylated regions, dense attachment was observed, such that it was difficult to distinguish individual particles. The mean height across the square, exposed regions was 40 nm for all four films, equal to the diameter of the NeutrAvidin particles, confirming that a monolayer formed.

dx.doi.org/10.1021/ja1103662 |*J. Am. Chem. Soc.* 2011, 133, 2749–2759

Nanofabrication. Nanofabrication was carried out by SNP. Light from the HeCd laser was coupled to a SNOM probe, and the probe was traced across the sample to deprotect lines of adsorbates. Before adsorbing NeutrAvidin particles, friction force microscopy (FFM)[74,75] was first used to characterize the features fabricated by SNP. FFM yields contrast due to changes in molecular composition[76−78] and packing.[79,80] Figure 6 shows FFM images of patterns fabricated by SNP, in which the exposed regions exhibit darker contrast (i.e., a smaller friction force) than the unmodified regions of surface. The contact angles measured for the OEG-functionalized surfaces were very similar to values obtained for deprotected amines, indicating that differences in surface adhesiveness are not likely to account for the friction contrast in figure 6. The OEG chains are lengthy, and likely to present multiple modes for the dissipation of energy in the sliding tip−sample interaction through tip-induced conformational change. This would be expected to raise the coefficient of friction, relative to the deprotected amines terminal groups, and probably accounts for the darker contrast (i.e., smaller friction forces) measured in the exposed regions.

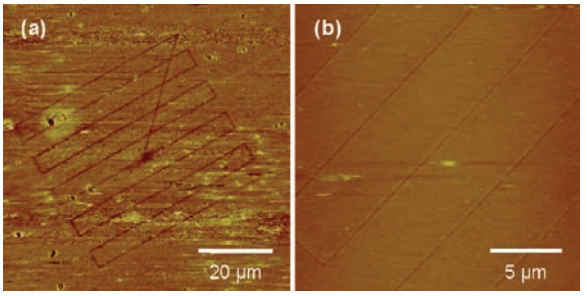

Figure 6. Friction force microscopy images of patterns formed in films of *m*-EG$_7$NPEOC by SNP. Vertical scale range: 0.0−0.5 mV dark to light (photodetector deflection).

The line width in Figure 6 was 180 nm. In the present case, commercially fabricated SNOM probes were used, and SEM characterization of the tips revealed that the width of the aperture was also ca. 180 nm, suggesting that the resolution is determined by the aperture dimensions. On the basis of previous work, we would thus expect smaller line widths to be feasible if probes with smaller apertures were used. Reducing the aperture diameter would also diminish the throughput of the probes, but the reduction in throughput would be nonlinear.[81] The reduction in throughput could be compensated by increasing the intensity of the laser beam coupled to the probe, or decreasing the writing rate, or, potentially, by the use of probes with a larger cone angle.[82,83]

Figure 7a and b shows patterns fabricated by SNP following derivatization with NHS-biotin, and then incubated in a solution of NeutrAvidin particles. To assist in relocating the nanopatterns after the ex situ bioconjugation steps, a micrometer-scale exposure was first carried out using an electron microscope "finder" grid to create patterns of larger features. These were visible in the optical microscope of the SNOM instrument, enabling the probe to be located with good precision adjacent to a particular registry

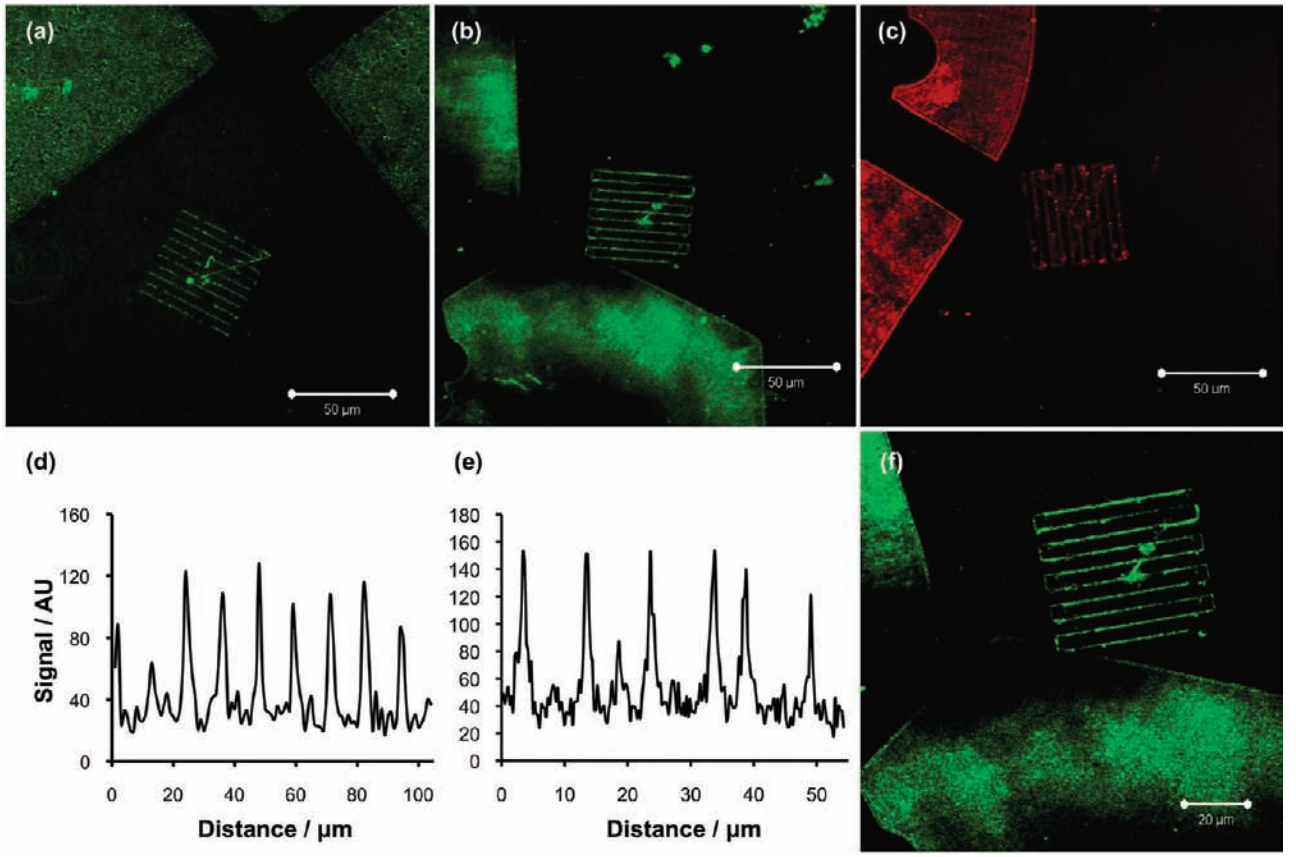

Figure 7. (a and b) Fluorescence micrographs showing NeutrAvidin nanopatterns formed by SNP adjacent to larger registry features formed using a mask-based process. Protecting groups: (a) *p*-EG$_4$NPEOC; (b) *p*-EG$_7$NPEOC. (c) AlexaFluor 647 conjugated streptavidin nanopattern formed in a film of of *p*-EG$_7$NPEOC-APTES. (d and e) Cross sections through the nanopatterns shown in (a) and (b), respectively. (f) Higher magnification image of the nanopattern formed in (b). Scale bars: 50 μm in (a)−(c) and 20 μm in (f).

dx.doi.org/10.1021/ja1103662 |*J. Am. Chem. Soc.* 2011, 133, 2749–2759

feature. After exposure of a region of intact adsorbates by SNP, the sample was removed, incubated in solutions of NHS-biotin followed by NeutrAvidin, and transferred to a confocal microscope for characterization. The microscale patterns are also readily located by confocal microscopy after avidin nanoparticle labeling, providing registry features to enable the nanopattern to be relocated easily.

Figure 7a−c shows low magnification images. The optical intensity of the nanolines was relatively low, because they were only ca. 4 NeutrAvidin particles wide, but they are nevertheless clearly visible even at this magnification. Figure 7c shows a pattern, formed by attachment of AlexaFluor 647-labeled streptavidin, demonstrating that the patterning method is equally efficacious for protein molecules, as opposed to protein-coated nanoparticles. Line sections through fluorescence images of the features yielded line widths somewhat larger than the widths obtained by FFM directly following SNP, due to the resolution limit of the confocal microscope (Figure 7d and e). Nevertheless, the line sections demonstrate that sharp, well-defined features have been formed. The full width at half-maximum (fwhm) was 340 nm in Figure 7d,e. The lenses used had numerical apertures of 1.3 and 1.4, meaning that the diffraction-limited resolution was ca. 229 and 213 nm, respectively. Given that the minimum width of the lines in the fluorescence image would be approximately equal to the actual line width plus the width of the point spread function, a fwhm of 340 nm is consistent with a protein line no larger than the features shown in Figure 6. AFM images did not enable an accurate determination of the feature size because of the crystallization of salt from the buffer solution onto the surface.

Strong fluorescence contrast was observed between the lines and the unexposed material on either side. The fluorescence signal does not reach zero anywhere in the image because of a low level of background intensity. However, given the strong signal in Figure 7f from the nanolines, which are only a few particles wide, one might expect any nonspecifically bound particles to be clearly evident. The absence of such features, apart from a very small number of isolated spots likely resulting from adventitious deposition, suggests that the NPEOC-protected film efficiently resists adsorption.

CONCLUSIONS

We have synthesized four photosensitive silanes possessing tetra- and hepta-ethylene glycol adducts at the *m*- or *p*- positions relative to the NPEOC group. In all cases, the nitrophenylethoxycarbonyl groups exhibit excellent sensitivity to irradiation at 325 nm, being extensively deprotected at an exposure of 2.24 J cm^{-2} to give an amine-functionalized surface, as revealed both by XPS measurements and by contact angle data for samples derivatized using TFAA. The XPS data show that for macroscopic UV exposures, all four adsorbates yield similar rates of photodeprotection. The potential use of this simple photoprotecting group strategy for carrying out surface modifications was demonstrated through the observation of highly efficient reactions with trifluoroacetic anhydride, with aldehyde-functionalized polymer nanoparticles, and with NHS-biotin, which facilitated the subsequent attachment of NeutrAvidin particles. All four adsorbates exhibited excellent resistance to nonspecific adsorption, and micropatterns yielded sharp fluorescence images with high contrast between masked and exposed regions. Near-field exposure also yielded photodeprotection of the adsorbates and facilitated fabrication of nanopatterns. The fluorescently labeled nanopatterns also exhibited excellent fluorescence contrast between exposed and unmodified regions. Overall, these data suggest that simple strategies based on the use of a PEGylated photocleavable protecting group offer great potential for the control of biological organization at micrometer and nanometer length scales. More generally, when integrated with near-field exposure methods, they hold great promise for the integration of synthetic chemical methodologies with nanofabrication, and for the ultimate unification of the top-down and bottom-up fabrication paradigms.

EXPERIMENTAL SECTION

Materials. The tetraethylene and heptaethylene glycol monomethyl ethers **1a** and **b** were purchased from ABCR (Karlsruhe, Germany) and TCI Europe (Zwijndrecht, Belgium) respectively. The 3-isocyanatopropyltriethoxysilane, trifluoroacetic anhydride (>99%), phosphate buffered saline (PBS), and (+)-biotin *N*-succinimidyl ester (>98% TLC) were supplied by Sigma-Aldrich (Poole, UK). Both methylnitrophenol isomers and all other reagents were purchased from Fisher Scientific (Loughborough, UK). The DMSO was dried over 3 Å molecular sieves prior to use. HPLC grade absolute ethanol was used as received. The Et_3N was dried over 4 Å molecular sieves for a minimum of 72 h prior to use. Tetrahydrofuran (THF), dimethylformamide (DMF), and toluene were supplied by a Grubbs dry solvent system. Aldehyde-coated 42 nm diameter nanoparticles (white aldehyde/sulfate polystyrene latex, 4% solids in suspension), NeutrAvidin conjugated yellow-green fluorescent (505/515) nanoparticles (1% solids) and AlexaFluor647-conjugated streptavidin were obtained from Invitrogen Molecular Probes (Paisley, UK). Immersol 518 F fluorescence free immersion oil and Citifluor glycerol/PBS solution mounting media were purchased from Carl Zeiss and Citifluor Ltd., respectively. Silicon (100) wafers were purchased from Goodfellow (Cambridge, UK).

Synthesis of Photolabile Silanes. Tosylation of both the glycols **1a** and **b** was effected with tosyl chloride according to previously described procedures.[68,69]

2-Nitro-4-(2,5,8,11-tetraoxatridec-22-yloxy)toluene, ***2a***. 4-Methyl-3-nitrophenol (689 mg, 4.5 mmol) and tosylate derivative of **1a** (1.5 g, 4.14 mmol) were dissolved in acetone (8 mL) and finely powdered K_2CO_3 (691 mg, 5 mmol) added. The suspension was heated under reflux at ca. 70 °C for 6 h, after which water (20 mL) was added and the mixture was extracted with Et_2O (15 mL twice). The organic layer was evaporated under reduced pressure, and the residue was purified by flash column chromatography (Hexanes:EtOAc, 1:1 → 1:4) to yield the desired **2a** as a yellow oil (1.29 g, 3.77 mmol, 91%); R_f 0.31 (Hex:EtOAc, 1:3); $\nu_{max}(BaF_2)/cm^{-1}$ 2875 (alkyl), 1529 (NO_2), 1349 (alkyl), 1249 (alkyl), 1107 (ether); δ_H (400 MHz, $CDCl_3$) 2.53 (3H, s, CH_3Ar), 3.38 (3H, s, CH_3O), 3.51−3.78 (12H, m, CH_2OCH_2), 3.88 (2H, t, *J* 4.8, CH_2CH_2OAr), 4.17 (2H, t, *J* 4.8, CH_2OAr), 7.10 (1H, d,d, *J* 2.5 and 8.5, 5-Ar), 7.23 (1H, d, *J* 8.5, 6-Ar), 7.54 (1H, d, *J* 2.5, 3-Ar); δ_C (100 MHz, $CDCl_3$) 19.7 ($ArCH_3$), 59.0 (CH_3O), 68.1, 69.5, 70.5, 70.6, 70.6, 70.9, 71.9 (all CH_2OCH_2), 110.0 (3-Ar), 120.5 (5-Ar), 125.7 (1-Ar), 133.4 (6-Ar), 149.34 (2-Ar), 157.3 (4-Ar); *m*/*z* (ES+) 344 (100%, $[M + H]^+$), 366 (60%, $[M + Na]^+$); HRMS found 344.1723, $[M + H]^+$ requires 344.1709, δ 4.1 ppm.

2-Nitro-5-(2,5,8,11-tetraoxatridec-22-yloxy)toluene, ***2b***. This compound was prepared using the procedure identical to that of **2a** except using 3-methyl-4-nitrophenol to yield **2b** as a brown oil (1257 mg, 3.66 mmol, 88%); R_f 0.25 (Hex:EtOAc, 1:3); $\nu_{max}(BaF_2)/cm^{-1}$ 2877 (alkyl), 1580 (aryl), 1511 (nitro), 1336 (alkyl), 1295 (alkyl), 1258 (alkyl), 1107 (ether); δ_H (400 MHz, $CDCl_3$) 2.63 (3H, s, CH_3Ar), 3.38 (3H, s, CH_3O), 3.51−3.79 (12H, m, CH_2OCH_2), 3.88 (2H, t, *J* 4.5, OCH_2CH_2OAr), 4.20, 2H, t, *J* 4.5, CH_2OAr), 6.80−6.85 (2H, m, 4 and 6-Ar), 8.08 (2H, d, *J* 8.6, 3-Ar); δ_C (100 MHz, $CDCl_3$) 21.6

dx.doi.org/10.1021/ja1103662 |*J. Am. Chem. Soc.* 2011, 133, 2749–2759

(CH_3Ar), 59.0 (CH_3O), 68.0, 69.4, 70.5, 70.6, 70.6, 70.9, 71.9 (all CH_2OCH_2), 112.3 (4-Ar), 118.1 (6-Ar), 127.5 (3-Ar), 137.0 (1-Ar), 142.3 (2-Ar), 162.3 (5-Ar); *m/z* (ES+) 344 (100%, $[M + H]^+$), 366 (30%, $[M + Na]^+$); HRMS found 344.1715, $[M + H]^+$ requires 344.1709, δ 1.7 ppm.

4-(2,5,8,11,14,17,20-Heptaoxadocosan-22-yloxy)-2-nitrotoluene, ***2c***. 4-Methyl-3-nitrophenol (612 mg, 4.0 mmol) and tosylate **1b** (865 mg, 1.75 mmol) were dissolved in acetone (10 mL), and finely powdered K_2CO_3 (691 mg, 5.0 mmol) was added. The suspension was refluxed at ca. 70 °C for 16 h, after which the solids were removed by filtration and the solution was evaporated under reduced pressure. The residue was purified by flash column chromatography (MeOH:DCM, 1:39 → 1:29) to yield the desired product as a pale yellow oil (737 mg, 1.55 mmol, 89%); R_f 0.29 (MeOH:DCM, 1:19); δ_H (500 MHz, $CDCl_3$) 2.52 (3H, s, CH_3Ar), 3.38 (3H, s, CH_3O), 3.55 (2H, t, *J* 3.0, $CH_3OCH_2CH_2$), 3.59−3.74 (22H, m, OCH_2CH_2O), 3.87 (2H, t, *J* 4.9, OCH_2CH_2OAr), 4.16 (2H, t, *J* 4.8, OCH_2CH_2OAr), 7.09 (1H, d,d, *J* 2.6 and 8.5, 5-Ar), 7.22 (1H, d, *J* 8.5, 6-Ar), 7.53 (1H, d, *J* 2.6, 3-Ar); δ_C (125 MHz, $CDCl_3$) 20.2 ($ArCH_3$), 59.4 (CH_3O), 68.4, 69.9, 70.9, 70.9, 71.0, 71.0, 71.3, 72.9 (all CH_2OCH_2), 110.3 (3-Ar), 120.9 (5-Ar), 126.1 (1-Ar), 133.8 (6-Ar), 149.6 (2-Ar), 157.7 (4-Ar); *m/z* (ES+) 476 (20%, $[M + H]^+$), 494 (100%, $[M + NH_4]^+$), 498 (15%, $[M + Na]^+$); found 476.2471, $[M + H]^+$ requires 476.2471, δ 0 ppm.

5-(2,5,8,11,14,17,20-Heptaoxadocosan-22-yloxy)-2-nitrotoluene, ***2d***. 3-Methyl-4-nitrophenol (612 mg, 4.0 mmol) and tosylate derivative of **1b** (1.5 g, 3.03 mmol) were dissolved in DCM (10 mL), and finely powdered K_2CO_3 (553 mg, 4.0 mmol) was added. The mixture was heated under reflux at ca. 50 °C for 16 h, after which the solids were removed by filtration and the solution evaporated under reduced pressure. The residual liquid was purified by flash column chromatography (MeOH: DCM, 49:1 → 1:24) to yield the desired product as a bright yellow oil (1.21 g, 2.55 mmol, 84%); R_f 0.22 (MeOH: DCM, 1:19); δ_H (400 MHz, $CDCl_3$) 2.62 (3H, s, CH_3Ar), 3.37 (3H, s, CH_3O), 3.50−3.76 (24H, m, OCH_2CH_2O), 3.87 (2H, t, *J* 4.6, OCH_2CH_2OAr), 4.18 (2H, t, *J* 4.6, OCH_2CH_2OAr), 6.78−6.83 (2H, m, 4,6-Ar), 8.07 (1H, d, *J* 9.6, 3-Ar); δ_C (100 MHz, $CDCl_3$) 22.1 ($ArCH_3$), 59.4 (CH_3O), 67.3, 69.8, 70.9, 70.9, 71.0, 71.0, 71.3, 72.3 (all CH_2OCH_2), 112.7 (4-Ar), 118.4 (6-Ar), 127.9 (3-Ar), 137.4 (1-Ar), 142.6 (2-Ar), 162.7 (5-Ar); *m/z* (ES+) 476 (10%, $[M + H]^+$), 493 (100%, $[M + NH_4]^+$), 498 (30%, $[M + Na]^+$); HRMS found 476.2498, $[M + H]^+$ requires 476.2490, δ 1.6 ppm.

2-[2-Nitro-4-(2,5,8,11-tetraoxatridec-22-yloxy)phenyl]ethanol, ***3a***. The pegylated nitrotoluene **2a** (1.72 g, 5.0 mmol) and paraformaldehyde (158 mg, 5.0 mmol) were suspended in DMSO (anhydrous, 6 mL) under an inert atmosphere. KO^{t}Bu (84 mg, 0.75 mmol) was added, and the mixture was stirred under an inert atmosphere at 85 °C for 1 h. The mixture was then neutralized with 0.05 M aqueous HCl (ca. 15 mL) and extracted with EtOAc (10 mL thrice). The organic layer was evaporated under reduced pressure and purified by flash column chromatography (EtOAc:EtOH, 1:0 → 4:1) to give the desired product as a yellow oil (654 mg, 1.75 mmol, 35%); R_f 0.39 (EtOAc:EtOH, 9:1); $\nu_{max}(BaF_2)$/cm^{-1} 3436 (hydroxy), 2877 (alkyl), 1530 (nitro), 1350 (alkyl), 1251 (alkyl), 1106 (ether); δ_H (400 MHz, $CDCl_3$) 1.69 (1H, s(br), O*H*), 3.10 (2H, t, *J* 6.0, $ArCH_2$), 3.38 (3H, s, CH_3O), 3.53−3.78 (12H, m, CH_2OCH_2), 3.80−3.99 (4H, m, OCH_2CH_2OAr and CH_2OH), 4.17 (2H, t, *J* 4.7, CH_2OAr), 7.13 (1H, dd, *J* 2.5 and 8.6, 5′-Ar), 7.31 (1H, d, *J* 8.6, 6′-Ar), 7.48 (1H, d, *J* 2.5, 3′-Ar); δ_C (100 MHz, $CDCl_3$) 35.9 ($ArCH_2$), 59.5 (CH_3O), 63.2 (CH_2OH), 68.5, 69.9, 70.9, 71.0, 71.3, 72.3 (all CH_2OCH_2), 110.6 (3-Ar), 120.7 (5-Ar), 126.2 (1-Ar), 134.0 (6-Ar), 150.3 (2-Ar), 158.2 (4-Ar); *m/z* (ES+) 374 (15%, $[M + H]^+$), 396 (100%, $[M + Na]^+$); HRMS found 396.1647, $[M + H]^+$ requires 396.1634, δ 3.3 ppm.

2-[2-Nitro-5-(2,5,8,11-tetraoxatridec-22-yloxy)phenyl]ethanol, ***3b***. The pegylated nitrotoluene **2b** (1.28 g, 3.7 mmol) and paraformaldehyde (113 mg, 3.7 mmol) were suspended in DMSO (anhydrous, 6 mL) under an inert atmosphere. KO^{t}Bu (63 mg, 0.56 mmol) was added, and the mixture was stirred under an inert atmosphere at 85 °C for 1 h. The mixture was then neutralized with 0.05 M aqueous HCl (ca. 15 mL) and extracted with EtOAc (10 mL thrice). The organic layer was evaporated under reduced pressure and purified by flash column chromatography (EtOAc:EtOH, 1:0 → 4:1) to give the desired product as a brown oil (465 mg, 1.24 mmol, 34%); R_f 0.33 (EtOAc:EtOH, 9:1); $\nu_{max}(BaF_2)$/cm^{-1} 3448 (hydroxy), 2879 (alkyl), 1514 (nitro), 1338 (alkyl), 1258 (alkyl), 1084 (ether); δ_H (400 MHz, $CDCl_3$) 1.84 (1H, s(br), O*H*), 3.21 (2H, t, *J* 6.2, $ArCH_2$), 3.38 (3H, s, CH_3O), 3.50−3.78 (12H, m, CH_2OCH_2), 3.88 (2H, t, *J* 4.5, OCH_2CH_2OAr), 3.95 (2H, td, *J* 6.0 and 5.5, CH_2OH), 4.21 (2H, t, *J* 4.5, CH_2OAr), 6.86 (1H, dd, *J* 9.0 and 2.5, 4-Ar), 6.91 (1H, d, *J* 2.5, 6-Ar), 8.05 (1H, d, *J* 9.0, 3-Ar); δ_C (100 MHz, $CDCl_3$) 37.5 ($ArCH_2$), 59.5 (CH_3O), 63.0 (CH_2OH), 68.5, 69.8, 70.9, 71.0, 71.3, 72.3 (all CH_2OCH_2), 113.4 (4-Ar), 118.7 (6-Ar), 128.2 (3-Ar), 137.6 (1-Ar), 142.9 (2-Ar), 162.7 (5-Ar); *m/z* (ES+) 374 (10%, $[M + H]^+$), 396 (100%, $[M + Na]^+$); HRMS found 396.1649, $[M + H]^+$ requires 396.1634, δ 3.8 ppm.

2-[4-(2,5,8,11,14,17,20-Heptaoxadocosan-22-yloxy)-2-nitrophenyl]-ethanol, ***3c***. The nitrotoluene **2c** (346 mg, 0.68 mmol) was mixed with paraformaldehyde (21 mg, 0.68 mmol) under an inert atmosphere, and DMSO (anhydrous, 2 mL) was added. KO^{t}Bu (7 mg, 0.06 mmol) was added and then stirred under an inert atmosphere at 80 °C for 30 min. The dark brown mixture was then quenched by the addition of 0.1 M aqueous HCl (20 mL) and extracted with DCM four times (10 mL each). The organic fractions were combined, dried with Na_2SO_4, and evaporated under reduced pressure. The residual oil was then purified by flash column chromatography (MeOH:DCM, 1:49 → 1:9) to give the desired product as a yellow liquid (86 mg, 0.17 mmol, 25%); R_f 0.10 (MeOH:DCM, 1:19); δ_H (400 MHz, $CDCl_3$) 3.07 (2H, t, *J* 6.4, $ArCH_2$), 3.35 (3H, s, CH_3O), 3.50−3.57 (2H, m, CH_2OCH_2), 3.58−3.75 (22H, m, CH_2OCH_2), 3.80−3.92 (4H, m, OCH_2CH_2OAr and CH_2OH), 4.15 (2H, t, *J* 4.4, CH_2OAr), 7.11 (1H, dd, *J* 2.4 and 8.4, 5-Ar), 7.29 (1H, d, *J* 8.8, 6-Ar), 7.45 (1H, d, *J* 2.8, 3-Ar); δ_C (100 MHz, $CDCl_3$) 35.5 ($ArCH_2$), 59.1 (CH_3O), 62.7 (CH_2OH), 68.1, 69.5, 70.5, 70.6, 70.6, 70.9, 71.9 (all CH_2OCH_2), 110.2 (3-Ar), 120.3 (5-Ar), 125.9 (1-Ar), 133.6 (6-Ar), 149.9 (2-Ar), 157.7 (4-Ar); *m/z* (ES+) 506 (35%, $[M + H]^+$), 523 (100%, $[M + NH_4]^+$), 528 (40%, $[M + Na]^+$); HRMS found 506.2578, $[M + H]^+$ requires 506.2601, δ 4.5 ppm.

2-[5-(2,5,8,11,14,17,20-Heptaoxadocosan-22-yloxy)-2-nitrophenyl]-ethanol, ***3d***. This compound was prepared using the same procedure as **3c** except using the pegylated nitrotoluene **2d**. The product was isolated as a yellow oil (103 mg, 0.20 mmol, 30%); R_f 0.14 (MeOH:DCM, 1:19); δ_H (400 MHz, $CDCl_3$) 2.52 (1H, s(br), O*H*), 3.20 (2H, t, *J* 6.2, $ArCH_2$), 3.37 (3H, s, CH_3O), 3.51−3.78 (24H, m, CH_2OCH_2), 3.87 (2H, t, *J* 4.6, OCH_2CH_2OAr), 3.95 (2H, t, *J* 6.2, CH_2OH), 4.21 (2H, t, *J* 4.6, CH_2OAr), 6.86 (1H, dd, *J* 2.8 and 8.8, 4-Ar), 6.92 (1H, d, *J* 2.8, 6-Ar), 8.04 (1H, d, *J* 8.8, 3-Ar); δ_C (100 MHz, $CDCl_3$) 37.0 ($ArCH_2$), 59.0 (CH_3O), 62.4 (CH_2OH), 68.0, 69.4, 70.4, 70.5, 70.6, 70.9, 71.9 (all CH_2OCH_2), 113.0 (4-Ar), 118.3 (6-Ar), 127.8 (3-Ar), 137.3 (1-Ar), 142.5 (2-Ar), 162.3 (5-Ar); *m/z* (ES+) 374 (10%, $[M + H]^+$), 396 (100%, $[M + Na]^+$); HRMS found 528.2420, $[M + Na]^+$ requires 528.2415, δ 0.9 ppm.

N-{2-[2-Nitro-4-(2,5,8,11-tetraoxatridec-22-yloxy)phenyl]ethoxy-carbonyl}-3-aminopropyltriethoxysilane, ***4a***. The pegylated nitrophenyl alcohol **3a** (167 mg, 0.43 mmol) was dissolved in DCM (2 mL), and to this was added 3-isocyanatopropyltriethoxysilane (129 mg, 0.52 mmol) followed by Et_3N (5.5 μL, 0.04 mmol). The solution was heated under reflux for 16 h and then evaporated under reduced pressure. The residual liquid was purified by flash column chromatography (Hex:EtOAc, 1:5 → 1:19) to yield the desired silane **4a** as a yellow oil (169 mg, 0.27 mmol, 63%); R_f 0.18 (Hex:EtOAc, 1:5); λ_{max}(EtOH)/nm 218 (ε/dm^3 $mol^{-1}cm^{-1}$ 16 974), 265 (3398), 330 (1995); $\nu_{max}(BaF_2)$/cm^{-1} 3344 (carbamate), 2883 (alkyl), 1721 (carbamate), 1531 (nitro), 1249 (silane), 1103, 1077 (ether

or siloxane); δ_H (400 MHz, $CDCl_3$) 0.60 (2H, t, *J* 8.5, CH_2Si), 1.22 (9H, t, *J* 6.5, CH_2CH_3), 1.52−1.65 (2H, m, $CH_2CH_2CH_2$), 3.10−3.23 (4H, m, $NHCH_2$ and $ArCH_2$), 3.38 (3H, s, CH_3O), 3.52−3.57 (12H, m, CH_2O), 3.81 (6H, q, *J* 7.0, $SiOCH_2$), 3.87 (2H, t, *J* 4.5, CH_2CH_2OAr), 4.17 (2H, t, *J* 4.5, CH_2OAr), 4.27 (2H, t, *J* 4.5, CH_2OCO), 4.87 (1H, s(br), NH), 7.11 (1H, dd, *J* 8.0 and 1.7, 5-Ar), 7.27 (1H, d, *J* 8.0, 6-Ar), 7.46 (1H, d, *J* 1.7, 3-Ar); δ_C (100 MHz, $CDCl_3$) 8.0 (CH_2Si), 18.7 (CH_2CH_3), 23.7 ($CH_2CH_2CH_2$), 32.4 ($ArCH_2$), 43.8 ($NHCH_2$), 58.9 ($SiOCH_2$), 59.5 (CH_3O), 64.6 (CH_2OCO), 68.5 (CH_2OAr), 69.9 (CH_2CH_2OAr), 70.9, 71.0, 71.3, 72.3 (all OCH_2), 110.6 (3-Ar), 120.6 (5-Ar), 125.6 (1-Ar), 133.7 (6-Ar), 150.6 (2-Ar), 156.6 (CO), 158.3 (4-Ar); *m*/*z* (ES+) 356 (100%, $[M - H_2O + H]^+$), 643 (55%, $[M + Na]^+$); HRMS found 643.2897, $[M + Na]^+$ requires 643.2874, δ 3.6 ppm.

N-{2-[2-Nitro-5-(2,5,8,11-tetraoxatridec-22-yloxy)phenyl]ethoxycarbonyl}-3-aminopropyltriethoxysilane, ***4b****.* The alcohol **3b** (251 mg, 0.67 mmol) was dissolved in DCM (2 mL), and 3-isocyanatopropyltriethoxysilane (193 mg, 0.78 mmol) and Et_3N (5.5 μL, 0.04 mmol) were added in succession. This mixture was heated under reflux for 16 h, the solvent evaporated under reduced pressure, and the residual oil purified by flash column chromatography (Hex:EtOAc, 1:5 → 1:19) to give the desired **4b** as an orange oil (259 mg, 0.42 mmol, 62%); R_f 0.15 (Hex:EtOAc, 1:5); λ_{max}(EtOH)/nm 232 (ε/dm^3 mol^{-1}cm^{-1} 7510), 303 (8258); ν_{max}/cm^{-1} 3340 (carbamate), 2885 (alkyl), 1722 (carbamate), 1516 (nitro), 1259 (silane), 1104, 1082 (ether or siloxane); δ_H (400 MHz, $CDCl_3$) 0.63 (2H, t, *J* 8.0, CH_2Si), 1.23 (9H, t, *J* 7.0, CH_2CH_3), 1.55−1.65 (2H, m, $CH_2CH_2CH_2$), 3.16 (2H, td, *J* 6.5 and 6.5, $NHCH_2$), 3.27 (2H, t, *J* 6.3, $ArCH_2$), 3.38 (3H, s, CH_3O), 3.53−3.77 (12H, m, CH_2O), 3.82 (6H, q, *J* 7.0, $SiOCH_2$), 3.88 (2H, t, *J* 4.5, CH_2CH_2OAr), 4.20 (2H, t, *J* 4.5, CH_2OAr), 4.32 (2H, t, *J* 4.5, CH_2OCO), 4.92 (1H, s(br), NH), 6.81−6.92 (2H, m, 4- and 6-Ar), 8.02 (1H, d, *J* 9.0, 3-Ar); δ_C (100 MHz, $CDCl_3$) 8.0 (CH_2Si), 18.7 (CH_2CH_3), 23.7 ($CH_2CH_2CH_2$), 33.9 ($ArCH_2$), 43.8 ($NHCH_2$), 58.9 ($SiOCH_2$), 59.5 (CH_3O), 64.4 (CH_2OCO), 68.5 (CH_2OAr), 69.8 (CH_2CH_2OAr), 70.9, 71.0, 71.3, 72.3 (all OCH_2), 113.3 (4-Ar), 118.5 (6-Ar), 128.0 (3-Ar), 136.8 (1-Ar), 145.6 (2-Ar), 156.6 (CO), 162.6 (5-Ar); *m*/*z* (ES+) 356 (100%, $[M - H_2O + H]^+$), 643 (50%, $[M + Na]^+$); HRMS found 643.2897, $[M + Na]^+$ requires 643.2874, δ 3.6 ppm.

N-{2-[2-Nitro-4-(2,5,8,11,14,17,20-heptaoxadocosan-22-yloxy)phenyl]ethoxycarbonyl}-3-aminopropyltriethoxysilane, ***4c****.* The alcohol **3c** (36 mg, 71 μmol) was dissolved in DCM (anhydrous, 3 mL), and 3-isocyanatopropyltriethoxysilane (46 μL, 184 μmol) was added, followed by Et_3N (2 μL, 14 μmol). The mixture was heated under reflux (ca. 60 °C) for 16 h. The mixture was evaporated under reduced pressure, and the residue was purified by flash column chromatography (MeOH:DCM, 1:49 → 1:19) to yield the title product as a pale yellow oil (35 mg, 46.5 μmol, 65%); R_f 0.29 (MeOH:DCM, 1:19); δ_H (400 MHz, $CDCl_3$) 0.60 (2H, t, *J* 8.2, CH_2Si), 1.20 (9H, t, *J* 7.0, CH_2CH_3), 1.59 (2H, tt, *J* 7.6 and 7.6, $CH_2CH_2CH_2$), 3.04−3.22 (4H, m, $NHCH_2$ and $ArCH_2$), 3.36 (3H, s, CH_3O), 3.53 (2H, t, *J* 4.6, $CH_3OCH_2CH_2O$), 3.55−7.73 (22H, m, CH_2OCH_2), 3.79 (6H, q, *J* 6.9, $SiOCH_2$), 3.85 (2H, t, *J* 4.6, CH_2CH_2OAr), 4.15 (2H, t, *J* 4.6, CH_2OAr), 4.25 (2H, t, *J* 6.4, CH_2OCO), 4.88 (1H, t(br), *J* 5.6, NH), 7.09 (1H, dd, *J* 2.8 and 8.8, 5-Ar), 7.24 (1H, d, *J* 8.0, 6-Ar), 7.43 (1H, d, *J* 2.4, 3-Ar); δ_C (100 MHz, $CDCl_3$) 7.6 (CH_2Si), 18.3 (CH_2CH_3), 23.3 ($CH_2CH_2CH_2$), 32.0 ($ArCH_2$), 43.4 ($NHCH_2$), 58.5 ($SiOCH_2$), 59.1 (CH_3O), 64.2 (CH_2OCO), 68.1 (CH_2OAr), 69.5 (CH_2CH_2OAr), 70.5, 70.6, 70.6, 70.6, 70.9, 71.9 (all OCH_2), 110.2 (3-Ar), 120.2 (5-Ar), 125.2 (1-Ar), 133.4 (6-Ar), 150.1 (2-Ar), 156.2 (CO), 157.8 (4-Ar); *m*/*z* (ES+) 771 (100%, $[M + NH_4]^+$, 776 (20%, $[M + Na]^+$); HRMS found 775.3645, $[M + Na]^+$ requires 775.3655, δ 1.3 ppm.

N-{2-[2-Nitro-4-(2,5,8,11,14,17,20-heptaoxadocosan-22-yloxy)-phenyl]ethoxycarbonyl}-3-aminopropyltriethoxysilane, ***4d****.* The alcohol **3d** (22 mg, 43 μmol) was dissolved in DCM (anhydrous, 100 μL), and Et_3N (21 μL, 100 μmol) was added followed by 4-nitrophenylchloroformate (30 mg, 149 μmol). The mixture was stirred in the dark, and after 24 h, all the alcohol was observed to be consumed by TLC together with the formation of a new product corresponding to the 4-nitrophenyl carbonate (R_f 0.40; MeOH:DCM, 1:19). EtOH (9 μL) was added, and the mixture was stirred for 10 min to quench the excess chloroformate. 3-Aminopropyltriethoxysilane (24 μL, 115 μmol) was added, and the reaction was observed to be complete by TLC after a further 24 h of stirring. The mixture was evaporated under reduced pressure, and the oily residue was purified by flash column chromatography (MeOH:DCM, 1:49 → 1:29) to yield the desired product (10 mg, 0.013 mmol, 30%); R_f 0.33 (MeOH:DCM, 1:19); δ_H (400 MHz, $CDCl_3$) 0.62 (2H, t, *J* 8.1, CH_2Si), 1.81 (9H, t, *J* 7.0, CH_2CH_3), 1.61 (2H, tt, *J* 7.4 and 7.8, $CH_2CH_2CH_2$), 3.11 (2H, dt, *J* 6.5 and 6.7, $NHCH_2$), 3.22 (2H, t, *J* 6.5, $ArCH_2$), 3.34 (3H, s, CH_3O), 3.51 (2H, t, *J* 4.6, $CH_3OCH_2CH_2O$), 3.53−3.72 (22H, m, CH_2OCH_2), 3.77 (6H, q, *J* 7.0, $SiOCH_2$), 3.84 (2H, t, *J* 4.7, CH_2CH_2OAr), 4.16 (2H, t, *J* 4.7, CH_2OAr), 4.28 (2H, t, *J* 6.5, CH_2OCO), 4.92 (1H, t(br), *J* 5.6, NH), 6.78−6.85 (2H, m, 4- and 6-Ar), 7.98 (1H, d, *J* 8.7, 3-Ar); δ_C (100 MHz, $CDCl_3$) 7.6 (CH_2Si), 18.3 (CH_2CH_3), 23.3 ($CH_2CH_2CH_2$), 33.5 ($ArCH_2$), 43.4 ($NHCH_2$), 58.4 ($SiOCH_2$), 59.0 (CH_3O), 63.9 (CH_2OCO), 68.1 (CH_2OAr), 69.4 (CH_2CH_2OAr), 70.5, 70.6, 70.6, 70.6, 70.9, 71.9 (all OCH_2), 113.0 (4-Ar), 118.1 (6-Ar), 127.6 (3-Ar), 136.4 (1-Ar), 142.7 (2-Ar), 156.3 (CO), 162.2 (5-Ar); *m*/*z* (ES+) 753 (10%, $[M + H]^+$), 770 (100%, $[M + NH_4]^+$), 775 (10%, $[M + Na]^+$); HRMS found 775.3658, $[M + Na]^+$ requires 775.3655, δ 0.4 ppm.

Film Preparation, Patterning, and Functionalization. Solutions (1 mM) of the isomers of NPEOC-APTES were prepared in dry toluene and chemisorbed on clean silicon oxide surfaces using previously published procedures.[47] Photodeprotection and patterning were conducted using a He−Cd laser (IK3202R-D, Kimmon, Tokyo, Japan), emitting at a wavelength of 325 nm. The samples of approximately 1.0 cm^2 were irradiated at a power of 11 mW with an area of irradiation of 1.77 cm^2. Masks consisting of 12.7 × 12.7 and 16.9 × 16.9 μm^2 square features were used for micrometer scale patterning. For SNP, the laser was coupled to an AlphaSNOM scanning near-field optical microscope (WiTec, Ulm, Germany). WiTec AlphaSNOM cantilever-type probes were used (WiTec, Ulm, Germany). The writing rate was 1 μm s^{-1}, meaning that it took ca. 50 s to write each of the lines in Figure 7.

After UV exposure, the reaction of the surface amine groups and TFAA was carried out in the presence of Et_3N. The samples were immersed in a 20 mM solution of the reagent in anhydrous tetrahydrofuran, with 40 mM triethylamine in Schlenck tubes under a dry N_2 atmosphere. Following the reaction, the derivatized samples were rinsed and sonicated in tetrahydrofuran for 10 min to remove any unreacted reagents. Following cleaning, the samples were blown dry with N_2 prior to further analysis.

Derivatization with aldehyde-functionalized nanoparticles was carried out by coating the micropatterned surface in a suspension of nanoparticles for 30 min (30 μL). The samples were then washed with ethanol and dried with nitrogen.

Biotin-terminated patterns were created on the amine surfaces using a solution consisting of biotin *N*-hydroxysuccinimide ester (10 mg mL^{-1}) in anhydrous dimethylformamide (DMF). The exposed films were cleaned, placed in a Schlenk tube, and purged with N_2. These samples were immersed in the biotin solution for 2 h, then removed and rinsed twice with DMF followed by ethanol, and finally dried with N_2 gas.

To attach NeutrAvidin beads to the biotinylted regions, NeutrAvidin bead suspension (10 μL) was mixed with phosphate buffered saline (PBS) solution (1 mL), and the patterned substrates were incubated for 2 h with the diluted suspension. For Alexa Fluor 647-conjugated streptavidin attachment, the same procedure was used, but in the final step a solution of the protein in PBS (10 μg mL^{-1}) was used in place of the NeutrAvidin suspension.

Surface Characterization. Contact angle measurements were made using a Rame-Hart model 100-00 water contact angle goniometer. For each sample, measurements were obtained at five different points on the surface of the samples, and the mean was calculated. The thicknesses of the films were obtained using a Jobin-Yvon UVISEL ellipsometer (Longjumeau, France). The measurements were performed at an incident angle of 70°, in the 200−850 nm spectral range. The Cauchy dispersion model used for fitting consists of a Si substrate coated with a layer of native SiO_2 and the NPEOC film.

Contact and tapping mode AFM imaging were performed using a Digital Instruments Nanoscope IIIa Multimode atomic force microscope (Veeco, Santa Barbara, CA). For contact mode imaging, silicon nitride probes (Nanoprobes, Veeco) with average spring constants 0.06 or 0.12 N m^{-1} and nominal tip radii between 20 and 60 nm were used. For tapping mode measurements, silicon probes with nominal force constants of 20−80 N m^{-1} were used.

X-ray photoelectron spectra were acquired on a Kratos Axis Ultra X-ray photoelectron spectrometer (Manchester, UK), operating at a base pressure of 1×10^{-9} mbar. Survey and high-resolution scans were acquired at pass energies of 160 and 80 eV, respectively. The Casa XPS software was used to analyze and curve-fit the spectra. The peaks were corrected relative to the C 1s hydrocarbon signal at a binding energy of 285.0 eV.

Fluorescence images were acquired with a LSM 510 Meta laser scanning confocal microscope (Carl Zeiss, Welwyn Garden City, UK). The samples were mounted in a glycerol/PBS-based anti fade solution (Citifluor AF1, Agar Scientific, UK) and observed with 40× and 63× oil immersion objectives (numerical apertures of 1.30 and 1.40, respectively). A small drop of immersion oil (Immersol 518 F, Zeiss) was placed on the slide in the center of the lighted area. All fluorescence images were analyzed using Zeiss LSM image browser software.

■ ASSOCIATED CONTENT

Ⓢ Supporting Information. Full citation for ref 45. This material is available free of charge via the Internet at http://pubs.acs.org.

■ AUTHOR INFORMATION

Corresponding Author

graham.leggett@shef.ac.uk; jason.micklefield@manchester.ac.uk

Present Addresses

[#]Department of Chemistry, Faculty of Science, Universiti Putra Malaysia, 43400 UPM Serdang, Selangor, Malaysia.

Author Contributions

[‖]These authors contributed equally.

■ ACKNOWLEDGMENT

We thank Research Councils UK (grant no. EP/C523857/1) for financial support. S.A.A.A. thanks the Malaysian Government for a research scholarship. L.S.W. gratefully acknowledges the EPSRC for the award of an LSI Fellowship (EP/F042590/1).

■ REFERENCES

(1) Piner, R. D.; Zhu, J.; Xu, F.; Hong, S.; Mirkin, C. A. *Science* **1999**, *283*, 661.

(2) Huo, F.; Zheng, Z.; Zheng, G.; Giam, L. R.; Zhang, H.; Mirkin, C. A. *Science* **2008**, *321*, 1658.

(3) Hong, S.; Zhu, J.; Mirkin, C. A. *Science* **1999**, *286*, 523.

(4) Demers, L.; Ginger, D. S.; Park, S.-J.; Li, Z.; Chung, S.-W.; Mirkin, C. A. *Science* **2002**, *296*, 1836.

(5) Lee, K.-B.; Park, S.-J.; Mirkin, C. A.; Smith, J. C.; Mrksich, M. *Science* **2002**, *295*, 1702.

(6) Amro, N. A.; Xu, S.; Liu, G.-Y. *Langmuir* **2000**, *16*, 3006–3009.

(7) Wadu-Mesthrige, K.; Amro, N. A.; Garno, J. C.; Xu, S.; Liu, G.-Y. *Biophys. J.* **2001**, *80*, 1891.

(8) Liu, G.-Y.; Amro, N. A. *Proc. Natl. Acad. Sci. U.S.A.* **2002**, *99*, 5165.

(9) Escalante, M.; Zhao, Y.; Ludden, M. J. W.; Vermeij, R.; Olsen, J. D.; Berenschot, E.; Hunter, C. N.; Huskens, J.; Subramaniam, V.; Otto, C. *J. Am. Chem. Soc.* **2008**, *130*, 8892.

(10) Wu, C.-C.; Reinhoudt, D. N.; Otto, C.; Velders, A. H.; Subramaniam, V. *ACS Nano* **2010**, *4*, 1083.

(11) Maoz, R.; Frydman, E.; Cohen, S. R.; Sagiv, J. *Adv. Mater.* **2000**, *12*, 725.

(12) Maoz, R.; Frydman, E.; Cohen, S. R.; Sagiv, J. *Adv. Mater.* **2000**, *12*, 424.

(13) Unruh, D. A.; Mauldin, C.; Pastine, S. J.; Rolandi, M.; Frechet, J. M. J. *J. Am. Chem. Soc.* **2010**, *132*, 6890.

(14) Ionescu, R. E.; Marks, R. S.; Gheber, L. A. *Nano Lett.* **2003**, *3*, 1639–1642.

(15) Takeda, S.; Nakamura, C.; Miyamoto, C.; Nakamura, N.; Kageshima, M.; Tokumoto, H.; Miyake, J. *Nano Lett.* **2003**, *3*, 1471–1474.

(16) Muller, W. T.; Klein, D. L.; Lee, T.; Clarke, J.; McEuen, P. L.; Schultz, P. G. *Science* **1995**, *268*, 272.

(17) Paxton, W. F.; Spruell, J. M.; Stoddart, J. F. *J. Am. Chem. Soc.* **2009**, *131*, 6692.

(18) Davis, J. J.; Coleman, K. S.; Busuttil, K. L.; Bagshaw, C. B. *J. Am. Chem. Soc.* **2005**, *127*, 13082.

(19) Fodor, S. P.; Read, J. L.; Pirrung, M. C.; Stryer, L.; Lu, A. T.; Solas, D. *Science* **1991**, *251*, 767.

(20) Pirrung, M. C.; Wang, L.; Montague-Smith, M. P. *Org. Lett.* **2001**, *3*, 1105.

(21) McGall, G. H.; Barone, A. D.; Diggelmann, M.; Fodor, S. P. A.; Gentalen, E.; Ngo, N. *J. Am. Chem. Soc.* **1997**, *119*, 5081.

(22) McGall, G.; Labadie, J.; Brock, P.; Wallraff, G.; Nguyen, T.; Hinsberg, W. *Proc. Natl. Acad. Sci. U.S.A.* **1996**, *93*, 13555.

(23) Singh-Gasson, S.; Green, R. D.; Yue, Y.; Nelson, C.; Blattner, F.; Sussman, M. R.; Cerrina, F. *Nat. Biotechnol.* **1999**, *17*, 974.

(24) Sun, S.; Chong, K. S. L.; Leggett, G. J. *J. Am. Chem. Soc.* **2002**, *124*, 2414.

(25) Sun, S.; Leggett, G. J. *Nano Lett.* **2004**, *4*, 1381.

(26) Montague, M.; Ducker, R. E.; Chong, K. S. L.; Manning, R. J.; Rutten, F. J. M.; Davies, M. C.; Leggett, G. J. *Langmuir* **2007**, *23*, 7328.

(27) Sun, S.; Montague, M.; Critchley, K.; Chen, M.-S.; Dressick, W. J.; Evans, S. D.; Leggett, G. J. *Nano Lett.* **2006**, *6*, 29.

(28) Sun, S.; Leggett, G. J. *Nano Lett.* **2007**, *7*, 3753.

(29) Tizazu, G.; Adawi, A.; Leggett, G. J.; Lidzey, D. G. *Langmuir* **2009**, *25*, 10746.

(30) Alang-Ahmad, S. A.; Hucknall, A.; Chilkoti, A.; Leggett, G. J. *Langmuir* **2010**, *26*, 9937.

(31) Hurley, C. R.; Ducker, R. E.; Leggett, G. J.; Ratner, B. D. *Langmuir* **2010**, *26*, 10203.

(32) Sun, S.; Mendes, P.; Critchley, K.; Diegoli, S.; Hanwell, M.; Evans, S. D.; Leggett, G. J.; Preece, J. A.; Richardson, T. H. *Nano Lett.* **2006**, *6*, 345.

(33) Iqbal, P.; Sun, S.; Hanwell, M. D.; Attwood, D.; Leggett, G. J.; Preece, J. A.; Richardson, T. H.; Tunnicliffe, D. *J. Mater. Chem.* **2008**, *18*, 2016.

(34) Haq, E. u.; Liu, Z.; Zhang, Y.; Ahmad, S. A. A.; Wong, L.-S.; Armes, S. P.; Hobbs, J. K.; Leggett, G. J.; Micklefield, J.; Roberts, C. J.; Weaver, J. M. R. *Nano Lett.* **2010**, *10*, 4375.

(35) Patchornik, A.; Amit, B.; Woodward, R. B. *J. Am. Chem. Soc.* **1970**, *92*, 6333.

(36) Sundberg, S. A.; Barrett, R. W.; Pirrung, M.; Lu, A. L.; Kiangsoontra, B.; Holmes, C. P. *J. Am. Chem. Soc.* **1995**, *117*, 12050.

(37) Beier, M.; Stephan, A.; Hoheisel, J. D. *Helv. Chim. Acta* **2001**, *28*, e11.

(38) Pirrung, M. C.; Huang, C.-Y. *Bioconjugate Chem.* **1996**, *7*, 317.
(39) Beier, M.; Stephan, A.; Hoheisel, J. D. *Helv. Chim. Acta* **2001**, *84*, 2089.
(40) Bhushan, K. R.; DiLisi, C.; Laurensen, R. A. *Tetrahedron Lett.* **2003**, *44*, 8585.
(41) Yang, Z.; Frey, W.; Oliver, T.; Chilkoti, A. *Langmuir* **1999**, *16*, 1751.
(42) Nakayama, K.; Tachikawa, T.; Majima, T. *Langmuir* **2008**, *25*, 6425.
(43) Alonso, J. M.; Reichel, A.; Piehler, J.; del Campo, A. *Langmuir* **2007**, *24*, 448.
(44) Wendeln, C.; Rinnen, S.; Schulz, C.; Arlinghaus, H. F.; Ravoo, B. J. *Langmuir* **2009**, *26*, 15966.
(45) Weinrich, D.; et al. *ChemBioChem* **2010**, *11*, 235.
(46) Orski, S. V.; Poloukhtine, A. A.; Arumugam, S.; Mao, L.; Popik, V. V.; Locklin, J. *J. Am. Chem. Soc.* **2010**, *132*, 11024.
(47) Alang-Ahmad, S. A.; Wong, L. S.; ul-Haq, E.; Hobbs, J. K.; Leggett, G. J.; Micklefield, J. *J. Am. Chem. Soc.* **2009**, *131*, 1513.
(48) Liu, M.; Amro, N. A.; Chow, C. S.; Liu, G.-Y. *Nano Lett.* **2002**, *2*, 863.
(49) Michel, R.; Reviakine, I.; Sutherland, D.; Fokas, C.; Csucs, G.; Danuser, G.; Spencer, N. D.; Textor, M. *Langmuir* **2002**, *18*, 8580.
(50) Park, S.-J.; Taton, T. A.; Mirkin, C. A. *Science* **2002**, *295*, 1503.
(51) Lee, K.-B.; Lim, J.-H.; Mirkin, C. A. *J. Am. Chem. Soc.* **2003**, *125*, 5588.
(52) Zhou, D. S. K.; Abell, C.; Rayment, T. *Angew. Chem., Int. Ed.* **2003**, *42*, 4934.
(53) Chow, D. C.; Lee, W.-K.; Zauscher, S.; Chilkoti, A. *J. Am. Chem. Soc.* **2005**, *127*, 14122.
(54) Rosi, N. L.; Mirkin, C. A. *Chem. Rev.* **2005**, *105*, 1547.
(55) Anker, J. N.; Hall, W. P.; Lyandres, O.; Shah, N. C.; Zhao, J.; Van Duyne, R. P. *Nat. Mater.* **2008**, *7*, 442.
(56) Gunnarsson, A.; Jonsson, P.; Marie, R.; Tegenfeldt, J. O.; Hook, F. *Nano Lett.* **2008**, *8*, 183.
(57) Graham, D.; Thompson, D. G.; Smith, W. E.; Faulds, K. *Nat. Nanotechnol.* **2008**, *3*, 548.
(58) Falconnet, D.; Koenig, A.; Assi, F.; Textor, M. *Adv. Funct. Mater.* **2004**, *14*, 749.
(59) Calvacanti-Adam, A. E.; Micoulet, A.; Blümmel, J.; Auernheimer, J.; Kessler, H.; Spatz, J. P. *Eur. J. Cell Biol.* **2006**, *85*, 219.
(60) Cavalcanti-Adam, E. A.; Volberg, T.; Micoulet, A.; Kessler, H.; Geiger, B.; Spatz, J. P. *Biophys. J.* **2007**, *92*, 2964.
(61) Malmstrom, J.; Christensen, B.; Jakobsen, J. P.; Lovmand, J.; Foldbjerg, R.; Sorensen, E.; Sutherland, D. S. *Nano Lett.* **2010**, *10*, 686.
(62) Harris, J. M. *Poly(Ethylene Glycol) Chemistry: Biochemical and Biomedical Applications*; Plenum: New York, 1992.
(63) Prime, K. L.; Whitesides, G. M. *Science* **1991**, *252*, 1164.
(64) López, G. P.; Ratner, B. D.; Tidwell, C.; Haycox, C.; Rapoza, R.; Horbett, T. *J. Biomed. Mater. Res.* **1991**, *26*, 415.
(65) Lopez, G. P.; Albers, M. W.; Schreiber, S. L.; Carroll, R.; Peralta, E.; Whitesides, G. M. *J. Am. Chem. Soc.* **1993**, *115*, 5877.
(66) Lopez, G. P.; Biebuyck, H. A.; Haerter, R.; Kumar, A.; Whitesides, G. M. *J. Am. Chem. Soc.* **1993**, *115*, 10774.
(67) Rosenhahn, A.; Schilp, S.; Kreuzer, H. J.; Grunze, M. *Phys. Chem. Chem. Phys.* **2010**, *12*, 4275.
(68) Snow, A. W.; Foos, E. E. *Synthesis* **2003**, 509.
(69) Delemarche, E.; Donzel, C.; Kamounah, F. S.; Wolf, H.; Geissler, M.; Stutz, R.; Schmidt-Winkel, P.; Michel, B.; Mathieu, H. J.; Schaumburg, K. *Langmuir* **2003**, *19*, 8749.
(70) Buhler, S.; Lagoja, I.; Giegrich, H.; Stengele, K.-P.; Pfleiderer, W. *Helv. Chim. Acta* **2004**, *87*, 620.
(71) Bhushan, K. R. *Org. Biomol. Chem.* **2006**, *4*, 1857.
(72) Eck, W.; Stadler, V.; Geyer, W.; Zharnikov, M.; Golzhauser, A.; Grunze, M. *Adv. Mater.* **2000**, *12*, 805.
(73) Golzhauser, A.; Eck, W.; Geyer, W.; Stadler, V.; Grunze, M. *Adv. Mater.* **2001**, *13*, 806.
(74) Overney, R.; Meyer, E. *MRS Bull.* **1993**, 26.
(75) Carpick, R. W.; Salmeron, M. *Chem. Rev.* **1997**, *97*, 1163.
(76) Frisbie, C. D.; Rozsnyai, L. F.; Noy, A.; Wrighton, M. S.; Lieber, C. M. *Science* **1994**, *265*, 2071.
(77) Chong, K. S. L.; Sun, S.; Leggett, G. J. *Langmuir* **2005**, *21*, 3903.
(78) Whittle, T. J.; Leggett, G. J. *Langmuir* **2009**, *25*, 9182.
(79) Beake, B. D.; Leggett, G. J. *Langmuir* **2000**, *16*, 735.
(80) Brewer, N. J.; Foster, T. T.; Leggett, G. J.; Alexander, M. R.; McAlpine, E. O. *J. Phys. Chem. B* **2004**, *108*, 4723–4728.
(81) Novotny, L.; Hecht, B. *Nanophotonics*; Cambridge University Press: Cambridge, UK, 2005.
(82) Lazarev, A.; Fang, N.; Luo, Q.; Zhang, X. *Rev. Sci. Instrum.* **2003**, *74*, 3679.
(83) Antosiewicz, T. J.; Szoplik, T. *Opto-Electron. Rev.* **2008**, *16*, 451.